

## Molecular-Dipole Deformation as a Collective Variable in Charge-Changing Ion-Atom Collisions

Jörg K. M. Eichler<sup>(a)</sup>

*Bereich Kern- und Strahlenphysik, Hahn-Meitner-Institut für Kernforschung Berlin GmbH,  
D-1000 Berlin 39, Federal Republic of Germany*

(Received 16 March 1981)

The molecular dipole moment along the internuclear line is treated as a collective coordinate to describe the sharing of electrons in slow atomic collisions. With use of the constrained Hartree-Fock method, potential energy surfaces for Li-F and (He-He)<sup>2+</sup> are calculated as a function of the internuclear separation and the dipole deformation. This offers a conceptual framework to view a charge-changing process as the motion along a path in the energy surface. Consequences for the molecular orbitals are discussed.

PACS numbers: 34.10.+x, 34.70.+e

Charge-state distributions in ion-atom collisions are defined at asymptotic internuclear separations  $R$ . For an extension to finite separations it is suggestive to introduce the electric dipole moment as a continuous "collective" variable to characterize the sharing of electrons between atoms or ions.<sup>1</sup> The introduction of collective degrees of freedom usually serves to separate some physically important gross features of the many-body system from the remaining "intrinsic structure." Within a molecular approach<sup>2</sup> charge-changing reactions may then be regarded as motions associated with the variation of  $R$  and the molecular dipole moment. The corresponding surfaces of total energy will provide some direct insight into the reaction and may furthermore serve as a first step towards a time-dependent Hartree-Fock (HF) treatment which has been developed in nuclear physics<sup>3</sup> to describe vibrating, rotating, and fissioning nuclei.

A static collective<sup>4</sup> state is generally represented as the lowest-energy state of a system *subject to a constraint force* which maintains a prescribed value of the collective amplitude. As the constraint force is a substitute for an inertial force which, according to d'Alembert's principle, balances the restoring force, the constraint operator is to be determined self-consistently.<sup>3</sup> In practice, however, it is more appropriate to define a "reasonable" constraint operator on the basis of physical intuition.

For a diatomic system, the operator for the dipole moment (divided by  $R/2$ ) along the internuclear line  $z$  (centered at the midpoint between the nuclei  $A$  and  $B$  and directed from  $A$  to  $B$ )

$$\hat{\zeta} = -\sum_i 2z_i/R + Z_B - Z_A \quad (1)$$

appears as a most suitable choice. The sum extends over all electrons. Atomic units are used

throughout. Correspondingly, we interpret the internuclear separation  $R$  and the dipole deformation  $\langle \hat{\zeta} \rangle$  (where the angular bracket denotes the many-body expectation value) as collective variables. Clearly,  $\langle \hat{\zeta} \rangle$  simply describes the charge difference between the two half-spaces separated by the midplane between the nuclei.

The constraint is imposed for a fixed  $R$  by minimizing, within a certain class of normalized trial functions, the expression<sup>5</sup>

$$\langle H \rangle - f(\lambda, \langle \hat{\zeta} \rangle), \quad (2)$$

where  $H$  is the many-body Hamiltonian,  $\lambda$  a constant, and  $f$  a differentiable function of  $\lambda$  and  $\langle \hat{\zeta} \rangle$ . After minimization for a given  $\lambda$  one obtains

$$E = \langle H \rangle, \quad \langle \hat{\zeta} \rangle = \zeta.$$

The method is implicit in that one first chooses a  $\lambda$ , minimizes the expression (2), and then finds for which  $\langle \hat{\zeta} \rangle$  the problem has been solved. The result is independent of the function  $f$ . Most commonly, one uses a linear constraint  $f_1 = \lambda \langle \hat{\zeta} \rangle$ , but if there is an inflection point in the curve  $E(\zeta)$  it is preferable to choose a quadratic constraint  $f_2 = C(\langle \hat{\zeta} \rangle - \lambda)^2$ . It is then possible to explore the whole energy surface  $E(R, \zeta)$  which forms a "landscape" above the  $(R, \zeta)$  plane with dips, valleys, and ridges. A collision process can be viewed as the motion along a path in this landscape. Since the initial system at  $R \rightarrow \infty$  is prepared with well-defined charge states  $k_A$  and  $k_B$  for target and projectile, the motion starts in a valley with  $\zeta = k_B - k_A$ . For low impact energies the collision path essentially follows the entrance valley until it merges into the molecular region where several valleys join together. The exit path is then determined by the details of the collision dynamics. The steepness or shallowness of a valley  $\zeta_0(R)$  is associated with the polarizabil-

ity along the internuclear line through the relation

$$\alpha_{\parallel} = [\partial^2 E(R, \zeta) / \partial \zeta^2]^{-1} (\frac{1}{2}R)^2, \quad (3)$$

which immediately follows from the interpretation<sup>1</sup> of a linear constraint force as  $R/2$  times the electric field needed to maintain the dipole deformation  $\zeta$ .

As illustrative examples, two energy landscapes are presented, one for the highly polar system Li-F and one for the homonuclear charged system (He-He)<sup>2+</sup>. A computer program for constrained HF calculations has been set up by modifying the BISON code<sup>6</sup> for diatomic molecules so as to include optionally a linear or a quadratic constraint. In each case more than 400 individual HF calculations were needed to build up a full energy surface.

For the Li-F system computations have been performed for the electronic configurations  $1\sigma^2 2\sigma^2 3\sigma^2 1\pi^4 4\sigma 5\sigma \Sigma$  and  $1\sigma^2 2\sigma^2 3\sigma^2 1\pi^4 4\sigma^2 1\Sigma$  (which correspond to atomic and ionic constituents, respectively) with use of an optimized<sup>7</sup> (12 $\sigma$ , 5 $\pi$ ) basis set of Slater-type orbital-molecular orbital (MO) wave functions. Figure 1 shows a contour map of the lowest-energy surface  $E(R, \zeta)$  with a stable minimum at  $R_e = 2.89$  a.u. and  $\zeta_e = 1.65$  (experimental values:  $R_e = 2.96$  a.u.,  $\zeta_e = 1.67$ ) and a saddle separating the atomic ( $\zeta = 0$ ) from the ionic ( $\zeta \approx 2$ ) valley. It is worth noticing that a conventional correlation diagram for the unconstrained energies  $E(R)$  would suggest a transition from the atomic to the ionic configuration to

occur at the *crossing point* of the energy curves while Fig. 1 suggests the energetically more favorable transition at the *saddle point*. Of course, with a more extended basis set than the one used here some of the details of the map will be modified, but the essence of the conclusions remains unchanged.

For the system (He-He)<sup>2+</sup> as a prototype of a charged collision system<sup>2</sup> computations have been performed for the configurations  $1\sigma^2 1\Sigma$  and  $1\sigma^2 2\sigma - \Sigma$  with use of a (16 $\sigma$ ) basis set optimized at  $R = 2$ . Because of the constraint, the molecule has no *gerade-ungerade* symmetry. As is well known, the unconstrained  $1\sigma_g^2$  system at  $R \rightarrow \infty$  dissociates into an unphysical mixture of He<sup>2+</sup>-He and He<sup>+</sup>-He<sup>+</sup> with an energy halfway in between. With a constrained HF approach one automatically obtains the physical solution He<sup>2+</sup>-He for large  $R$  if  $\zeta \geq 2$  (as may be verified by inspection of the wave function). But as soon as  $\zeta$  is decreased below 2, the MO wave function lowers its energy by admixing (unphysical) covalent He<sup>+</sup>-He<sup>+</sup> terms. In Fig. 2 we therefore have for  $R \geq 4$  and  $\zeta < 2$  substituted the atomic constituents: He polarized by a charge  $Z_B = 2$  near  $\zeta = 2$  and He<sup>+</sup> polarized by a charge  $Z_B = 1$  (scaled to two ions) near  $\zeta = 0$ . The height of the ridge between the valleys at  $\zeta = 0$  and  $\zeta = 2$  is derived from the He<sup>+</sup>-He<sup>+</sup> potential barrier.

While the potential-energy surfaces just discussed may be helpful in visualizing a charge-changing process they do not, by themselves, provide a simple guide to the dynamical motion of the system through the  $(R, \zeta)$  plane. In order to treat the collective motion the time-dependent

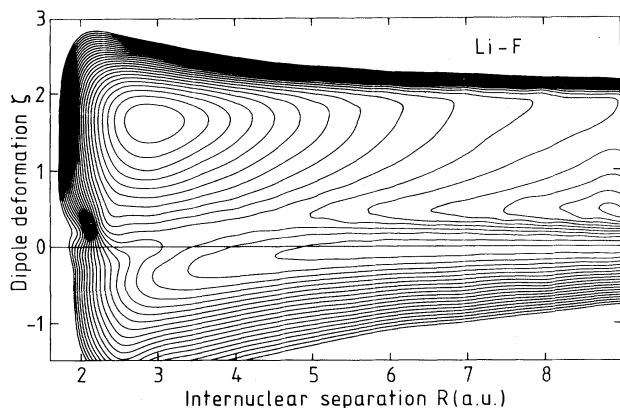


FIG. 1. Contour map of the potential energy landscape  $E(R, \zeta)$  for Li-F. The lowest contour line in the atomic valley at  $\zeta = 0$  corresponds to the energy  $-106.82$  a.u. Successive lines are separated by  $\Delta E = 0.02$  a.u. The minimum in the ionic valley  $\zeta \approx 2$  has  $E_e = -106.976$  a.u.

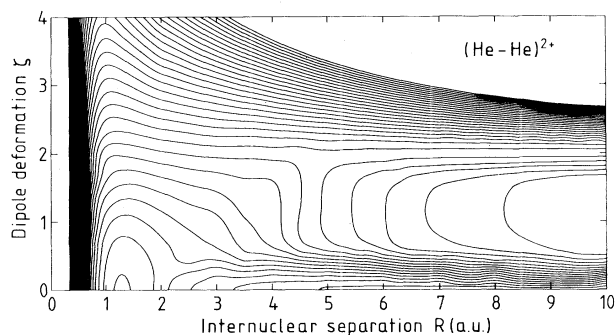


FIG. 2. Contour map of the potential-energy surface  $E(R, \zeta)$  for (He-He)<sup>2+</sup>. Because of the symmetry with respect to  $\zeta \rightarrow -\zeta$  only the part for  $\zeta \geq 0$  is shown. The lowest contour line in the valley at  $\zeta = 2$  corresponds to the energy  $-2.80$  a.u. Successive lines are separated by  $\Delta E = 0.1$  a.u.

state,  $\varphi(t)$  is assumed to follow a trajectory parametrized by  $\vec{R}(t)$  and  $\xi(t)$  and by the associated momenta  $\vec{P}(t)$  and  $p_\xi(t)$  so that  $\varphi(t) = \varphi(\vec{R}, \xi; \vec{P}, p_\xi)$ . Then the energy functional

$$\mathcal{H}(\vec{R}, \xi; \vec{P}, p_\xi) = \langle \varphi(t) | H | \varphi(t) \rangle \quad (4)$$

can be interpreted as a classical collective Hamiltonian.<sup>3,8</sup> It is composed of the potential  $V(R, \xi) = E(R, \xi)$  calculated before and the kinetic energy which in the adiabatic limit contains only second-order diagonal terms in the momenta (the Born-Oppenheimer approximation rules out mixed terms in  $\vec{P}$  and  $p_\xi$ ). Thus

$$\mathcal{H} = P^2/2\mu + p_\xi^2/2M(R, \xi) + V(R, \xi), \quad (5)$$

where  $\mu$  is the ion-atom reduced mass and  $M(R, \xi)$  the inertial parameter corresponding to the motion in  $\xi$ . An approximate value for this quantity is given by the so-called cranking formula<sup>9</sup>

$$M(R, \xi) = 2 \sum_{p-h} |\langle p-h | \partial/\partial\xi | \varphi \rangle|^2 / (e_p - e_h). \quad (6)$$

Here p-h denotes a particle-hole configuration (with energy  $e_p - e_h$ ) excited from the deformed Slater determinant  $\varphi$ . It is noted that  $M$  increases proportional to  $R^2$  while the valleys of stability in  $V(R, \xi)$  become narrower and steeper. Once the inertial parameter is known the classical collective motion is determined by the canonical equations  $\dot{\xi} = \partial\mathcal{H}/\partial p_\xi$  and  $\dot{p}_\xi = -\partial\mathcal{H}/\partial\xi$  (and similar equations for  $\vec{R}$  and  $\vec{P}$ ). One then may go a step further<sup>3</sup> and "requantize" the system via the familiar substitution for the kinetic energies in Eq. (5).

The adiabatic approach implied in Eqs. (4)–(6) has been shown<sup>3,8</sup> to be good as long as the collective kinetic energy  $p_\xi^2/2M$  per particle involved is small compared to typical single-particle excitation energies. Assuming that  $p_\xi^2/2M$  is of the same order as typical variations of  $V(R, \xi)$  this condition appears to be satisfied in the two cases considered. A full treatment of the dynamics will also have to address the problem of damping and of couplings between the collective and the single-particle motion.

The single-particle states associated with a potential-energy landscape are uniquely determined by the two-parameter family of Slater determinants forming the constrained HF ground state. For adiabatic or near-adiabatic charge-changing collisions the process more or less follows (depending on the dynamics) the energetically lowest possible path  $\xi_0(R)$ . It is along this path that the corresponding single-particle states

are most adequate for an MO description during the collision. In fact, these MO's describe approximately independent electrons because an important part of the electron correlations (namely that part governing the charge transport through the midplane between the nuclei) has been incorporated in the deformed Slater determinant  $\varphi(R, \xi)$ . This is analogous to the situation in nuclear physics where deformed or superfluid nuclei generate their own, approximately non-interacting, quasiparticle states.

The MO energies displayed in conventional correlation diagrams have hence to be identified with single-electron energies (which are expectation values of the HF operator with respect to constrained MO's) taken along a suitable path. Regarded as functions of  $R$  alone they have a remarkable feature<sup>1</sup>: *Energy curves of MO's with like symmetries can cross under certain conditions*. After all, this is not so surprising for a two-parameter family of states. Non-self-consistent model calculations<sup>10</sup> indeed show such crossings. Their existence also seems to be confirmed by recent experiments<sup>11</sup> on the  $K$ -vacancy production in collisions of 50–250-keV  $C^{n+}$ ,  $N^{n+}$ ,  $O^{n+}$  ( $n=1, 2, 3$ ) with Ne. Contrary to common expectation that the  $2p\pi$  MO should correlate to the energetically lower (ionized)  $2p$  state of  $C^{n+}$ ,  $N^{n+}$ ,  $O^{n+}$ , the data show that it correlates instead to the energetically higher  $2p$  state of Ne. This indicates a crossing of  $2p\pi$  and  $3d\pi$  MO's.

In conclusion, I believe that the energy landscapes  $E(R, \xi)$  open up a new way to visualize slow charge-changing atomic collisions, particularly with *multiply charged ions* offering access to a wide range of  $\xi$  values. They also provide a pictorial measure of the ionic (Fig. 1) or covalent (Fig. 2) character of diatomic molecules. A generalization to polyatomic molecules can be achieved by choosing a constraint operator suited to the geometry. It still will require considerable effort to further implement the ideas advanced here and to sharpen them to a quantitative method for treating the dynamics of charge-changing atomic collisions.

I am indebted to F. J. de Heer and F. W. Saris for reviving my interest in the problem, to H. J. Krappe and J. H. McGuire for useful discussions, and to N. Stolterfoht for initial advice in use of the BISON code. I owe thanks to Miss D. Schoening for her help in computer handling.

<sup>(a)</sup>Also at Fachbereich Physik, Freie Universität

Berlin, D-1000 Berlin 39, Federal Republic of Germany.

<sup>1</sup>J. Eichler, Phys. Rev. Lett. **40**, 1560 (1978), and to be published.

<sup>2</sup>W. Lichten, Phys. Rev. **131**, 229 (1963), and **139**, A27 (1965); U. Fano and W. Lichten, Phys. Rev. Lett. **14**, 627 (1965).

<sup>3</sup>F. Villars, Nucl. Phys. **A285**, 269 (1977).

<sup>4</sup>For an application of collective states to nuclear fission, see, e.g., S. Bjørnholm and J. E. Lynn, Rev. Mod. Phys. **52**, 725 (1980).

<sup>5</sup>H. Flocard, P. Quentin, A. K. Kerman, and D. Vautherin, Nucl. Phys. **A203**, 433 (1973).

<sup>6</sup>A. C. Wahl, P. J. Bertocini, K. Kaiser, and R. H. Land, Argonne National Laboratory Report No. ANL-7271, 1968 (unpublished).

<sup>7</sup>A. D. McLean, J. Chem. Phys. **39**, 2653 (1963); set VIII.A was used.

<sup>8</sup>M. Baranger and M. Vénéroni, Ann. Phys. (N.Y.) **A114**, 123 (1978).

<sup>9</sup>D. R. Inglis, Phys. Rev. **96**, 1059 (1954), and **97**, 701 (1955).

<sup>10</sup>J. Eichler, W. Fritsch, and U. Wille, Phys. Rev. A **20**, 1448 (1979).

<sup>11</sup>P. H. Woerlee, N. W. de Waard, and F. W. Saris, J. Phys. B **13**, 2965 (1980).

## Z Dependence of Bremsstrahlung Radiation from Free Atoms

R. Hippler,<sup>(a)</sup> K. Saeed, I. McGregor, and H. Kleinpoppen

*Institute of Atomic Physics, University of Stirling, Stirling FK9 4LA, Scotland*

(Received 22 April 1981)

Relative bremsstrahlung cross sections have been measured for free atoms, with atomic numbers in the range  $Z=2$  to  $Z=92$ , at low incident electron energies of 2.5 and 10 keV. The results agree reasonably with a theoretical calculation of Pratt *et al.*, except at the largest  $Z$  number, where differences of up to a factor of 2 at low photon energies are observed.

PACS numbers: 34.80.-i

Electrons being accelerated in the fields of neutral or ionized atoms give rise to the emission of noncharacteristic radiation. This atomic field bremsstrahlung is of fundamental importance as well as of practical relevance for various plasma and fusion projects and in biological applications.<sup>1</sup>

Most modern discussions of bremsstrahlung radiation start with the work of Sommerfeld and co-workers.<sup>2-4</sup> In a nonrelativistic, quantum-mechanical calculation, Sommerfeld and Maue<sup>3</sup> obtained  $d\sigma/dk$ , the bremsstrahlung cross section differential in photon energy  $k$ ,

$$\frac{d\sigma}{dk} = \frac{16\pi^2}{3} \alpha^5 a_0^2 \frac{Z^2}{k\beta_1^2} \frac{x_0}{[\exp(2\pi n_1) - 1][1 - \exp(-2\pi n_2)]} \frac{d}{dx_0} |F(x_0)|^2, \quad (1)$$

with  $n_{1,2} = \alpha Z / \beta_{1,2}$ ,  $\beta_{1,2} = v_{1,2}/c$ ,  $v_{1,2}$  the ingoing and outgoing electron velocity,  $a_0$  the Bohr radius,  $x_0 = -4n_1 n_2 / (n_1 - n_2)^2$ , and  $F = F(in_1, in_2, 1, x_0)$  the hypergeometric function. At low incident electron energies  $T$  ( $T \leq 10$  keV) this result is almost identical to a relativistic calculation of Elwert and Haug.<sup>5</sup> For sufficiently large energies  $2\pi n_{1,2} \ll 1$ , Eq. (1) reduces to

$$d\sigma/dk = \frac{8}{3} \alpha^5 a_0^2 (Z^2/k\beta_1^2) \ln(1 - x_0). \quad (2)$$

Equation (2) predicts a  $Z^2$  dependence of bremsstrahlung cross section.

Here we report on an investigation of the  $Z$  dependence of bremsstrahlung cross section  $d\sigma/dk$  for the electron bombardment of free (gaseous) atoms at low incident electron energies ( $T = 2.5$

to 10 keV). The results are compared with a recent numerical calculation of Pratt *et al.*<sup>6</sup> in which the screening of the nuclear field by the surrounding electrons is taken into account.

The experimental arrangement has been described in detail previously.<sup>7</sup> It consists essentially of an electron gun inside a vacuum chamber, providing beam currents of about 100  $\mu\text{A}$ . Gas is introduced into the chamber through a needle valve producing a pressure typically about  $1 \times 10^{-3}$  mbar for all gases studied with the exception of helium. In the case of helium, pressures up to  $4 \times 10^{-3}$  mbar have been used. A Baratron capacitance manometer was used for the pressure measurements. X rays produced by the col-